The LAPS Wind Analysis

by

Steven C. Albers*

Forecast Systems Laboratory
Boulder, Colorado

---

* Jointly affiliated with the Cooperative Institute for Research in the Atmosphere, Colorado State University, Fort Collins, CO.

Corresponding author address: Steven C. Albers, Forecast Systems Laboratory, NOAA/FSL, R/E/FS1, 325 Broadway, Boulder CO 80303-3328, E-mail: albers@fsl.noaa.gov.

ABSTRACT

The Local Analysis and Prediction System (LAPS) wind analysis combines Doppler radar, profiler, aircraft, and surface wind observations into a three-dimensional gridded wind field. Other fields derived primarily from the wind analysis include radar echo steering wind, helicity, and Lifted Index (LI) times vertical velocity (an indicator of convective potential). This report describes LAPS wind analysis procedures. The goal is to combine various data sources to take advantage of the strengths of each source, thereby automating the data synthesis that a human forecaster performs. The utility of these analyses to the operational forecaster is an important part of designing the analysis procedure and output displays. Comparisons of LAPS wind fields with independent aircraft measurements obtained during the Winter Icing and Storms Project (WISP) experiment indicate agreement generally within 4 m s^{-1} (rms).

1. Introduction

New data sources available at the Forecast Systems Laboratory (FSL), one of the National Oceanic and Atmospheric Administration's Environmental Research Laboratories, are being used to develop new types of mesoscale analyses. FSL's Local Analysis and Prediction System (LAPS; McGinley et al. 1991) produces hourly analyses with a grid resolution of 10 km horizontally and 50 hPa vertically. The domain currently covers northeastern Colorado as well as parts of adjoining states. LAPS analyses of temperature, moisture, pressure, winds, clouds, and precipitation are being developed. The procedures used for analyzing these and other derived fields on this and finer scales are unique aspects of LAPS.

The datasets ingested in real time in the Colorado domain (Fig. 1) are similar to those to be collected in the near future by data networks being deployed in many other areas. This presents a unique opportunity to develop operational local assimilation and processing systems that can cope with the anticipated flood of data, and that will help weather services meet the goal of improved forecasts in the 0-6 h period.

2. Datasets used in LAPS

FSL has supported a unique real-time data ingest facility for many years. The data collected routinely include the following:

- Surface observations at 22 local sites every 5 min, as well as hourly surface aviation observations (SAOs) from North America.
- Doppler radar volume scans at 6-min intervals.
- Wind and temperature Radio Acoustic Sounding System (RASS) profiles from the NOAA Demonstration Profiler Network (60-min interval).
- Satellite visible data (5- or 30-min interval) and multichannel image and sounding data (90-min interval).
- Automated reports from selected aircraft at random times.

These data are roughly comparable to what will be available at most weather offices by the late 1990s. We can conservatively expect that within a 300-km radius of many Weather Forecast Offices (WFOs), there will be 25 SAOs and ASOSs (Automated Surface Observing Systems), one or more Doppler radars, one or more wind profilers, ACARS (Aeronautical Radio Incorporated, Communications and Retrieval System) aircraft observations, and a variety of satellite data. Thus we designed a data assimilation and analysis system compatible with this data configuration.

The wind analysis (example in Fig. 2) combines Doppler weather radar, profiler, aircraft, and surface wind data into a three-dimensional wind field. Other fields derived primarily or in part from the wind analysis include echo steering wind, helicity, and Lifted

Index (LI) times vertical velocity (an indicator of convective potential). The analyzed fields reside in a 10-km horizontal, 50 hPa vertical grid having dimensions of 61 x 61 x 21, and are being produced in real time at 60-min intervals.

Most of the fields described herein are being generated in real time and are available for inspection on meteorological workstations at FSL and at the WFO located in Denver, Colorado. Based on our examination of these fields in real time, we believe that a local, high-resolution, gridded database will be a valuable resource within the WFO. It will allow forecasters to quickly update their knowledge of the structure of the atmosphere within their region of responsibility by inspecting two- and three-dimensional graphical displays, animating these displays on a workstation, diagnosing dynamically relevant derived quantities that have forecast application, and interacting with the database to develop new forecast methods and products.

3. Radar reflectivity and radial velocity analyses

Because radar data (particularly velocities) are a novel and important input into the wind analysis package, it is appropriate to describe how these data are preprocessed and remapped onto the LAPS grid. The gate-by-gate radar data are processed by the FSL real-time Doppler products subsystem (Lipschutz et al. 1989). A real-time program was run that generated three-dimensional Cartesian gridded radial velocities and reflectivity factors for each volume scan of Mile-High Radar, located 20 km northeast of Denver, Colorado. Mile-High Radar is a modified NEXRAD (Next Generation Radar) prototype operating at 10-cm wavelength and 250-m gate velocity gate spacing (Pratte et al. 1991). The radar employs a V-notch clutter filter, a spike removal filter, and a map to suppress much of the ground clutter. An additional clutter-screening step involves removing any velocity gate having a magnitude of <2 m s^{-1}. Mile-High Radar has no velocity dealiasing capability. Velocity data coverage extends up to 150 km from the radar, depending on the scattering characteristics of the air and various types of meteors.

To prevent range aliasing, reflectivity data for low elevation angles are taken from long range scans (to 460 km) with reduced pulse repetition frequency (PRF). For the velocities, reflectivity scans are compared at two different PRFs (unambiguous ranges of 460 km and 150 km), thereby flagging range-folded velocity data. If the flag indicates good data, the radial velocity from the short range scan is used. The nyquist folding velocity in the short range scan is 26 m s^{-1}.

For each LAPS grid point, the remapping algorithm computes reflectivity by taking the mean dBZ value of all gates within a grid volume centered on the LAPS grid point. Current computer limitations do not allow experimenting with other types of averaging (such as mean Z_e, where $Z_e = 10log_{10}dBZ$). When the mean reflectivity is less than 0 dBZ, it is set to a flag value of -10 dBZ, thus avoiding problems with electronic noise and non-hydrometeor scatterers.

The radial velocity is averaged similarly. Several quality checks are performed on the velocity data. One requirement is that $>40\%$ of all gates located within a LAPS grid

box or at least 4 of them, whichever is greater, must contain valid velocity data (i.e., are not flagged as ground clutter or range-folded). Another check is done on the standard deviation of the velocities. If a threshold is exceeded, the LAPS grid box is assigned the missing data value. It should be noted that broad volumetric coverage of quality controlled velocity data is contingent upon there being sufficient scattering particles present in the atmosphere.

The data are written in arrays containing only those bytes having valid velocity values, thus saving much disk space. A subroutine reads these packed radar files and decompresses the radar data. This radar reading subroutine uses an option to apply an additional three-dimensional Cartesian ground clutter map to the reflectivity data. This fixed clutter map resides in the LAPS grid and consists of the maximum reflectivity in each LAPS grid volume from several clear-air volume scans. When the clutter map is applied, any observed reflectivity not exceeding the clutter map by 10 dBZ is set to the base value of -10 dBZ (no meteorological echo).

For reflectivity, another subroutine fills in gaps of up to three vertical levels using linear interpolation. This is to allow for the space between successive radar sweeps with increasing antenna elevation at distant ranges. The routine also has the option of filling in echo in low levels judged to be either below the radar horizon (due to the earth's curvature) or blanked out by mountains or ground clutter. Any reflectivity echo whose base is within two LAPS grid levels (100 hPa) of the local terrain is assumed by the fill routine to extend down to the ground in reality.

The volumetric coverage of reflectivity data is subjected to a temporal continuity test. If the number of valid reflectivity grid volumes differs by more than a preset, empirically determined threshold (300) between successive volume scans, the later scan is flagged as bad. A single bad volume scan (often occurring near startup) may thus cause two successive scans to be flagged as bad.

Among the fields derived from the radar analysis are echo top height and a 1-h forecast of echo location based on layer mean winds. Layer mean winds are calculated from the surface to 300 hPa as described in Section 5b. The echoes for this field are advected with a surface to 300 hPa layer mean wind speed, except near convective storms, where storm-tracking vectors are utilized.

An additional way to present radar data involves identifying the maximum reflectivity in a given LAPS grid column over the duration of the 1-h analysis cycle. This maximum reflectivity field is being utilized in the analysis of a summer forecasting experiment called Z-Cast91 held at FSL (Jackson and Albers 1992).

4. Wind analysis procedure

The wind analysis procedure for the u and v wind components uses all available data sources in a two-pass objective analysis, as illustrated in the flow chart (Fig. 3). Wind information tangential to the radar beam comes initially from the nonradar data. These

tangential winds are merged with the radar radial velocities to provide full two-dimensional wind vectors at the location of each radial velocity measurement.

In the first pass (looping clockwise in Fig. 3) SAOs, surface mesonet, profiler, and aircraft reports are used to generate a preliminary analysis. Time tendencies from the Mesoscale Analysis and Prediction System (MAPS; Benjamin et al. 1991) are utilized to update the aircraft reports because these can be nearly 1 h old, exceeding the LAPS analysis cycle time. MAPS is a 60 km resolution isentropic analysis and forecast model being developed at FSL and field tested and the National Meteorological Center. The profiler data are also updated because the center of the 1-h averaging period is 30-min offset with respect to the analysis time. The time tendency is calculated by taking the difference of MAPS forecasts valid at the current and previous LAPS cycle times. Six-hour MAPS forecasts are interpolated both spatially and temporally to the LAPS grid, representing the shortest forecast period for which MAPS data are consistently available in real time. (Restrictions imposed by the MAPS 3-h assimilation cycle preclude the regular availability of MAPS analyses or 3-h forecasts). A background wind analysis is subtracted from the new observations to produce observation residuals. Either MAPS winds or the previous hour's LAPS wind (persistence forecast) can be used as a background field. There are advantages and disadvantages to either approach, as described next.

The use of LAPS as a background provides for time continuity, but one based largely on persistence. This is a type of four-dimensional data assimilation, as a given datum retains its effect over several analysis cycles, depending on future data density in the same region. A long-term goal is to make LAPS more self-contained by incorporating a prognostic component to provide the background field. A major drawback with the LAPS persistence field approach is that erroneous data values occurring in data-sparse regions can cause perturbations that persist in the analysis for many cycles. As a result, the MAPS background is currently used in our real-time system. Drawbacks to this method are potential inaccuracies due to errors in the MAPS forecasts or because of potential inaccuracies arising from the temporal and spatial interpolation of the coarser MAPS forecast values to the LAPS grid points. We are starting to experiment with using a mesoscale model forecast (initialized with previous LAPS analyses) as the background in a four-dimensional assimilation scheme (Sec. 9).

Time windows are applied to the observations as follows. For the mesonet data, the 5-min average ending at analysis time is used. Surface aviation observations are taken hourly, typically about 10 min before analysis time. Profiler data, available hourly, are averaged for 60 min before the stated analysis time; they are used only for analyses done on the hour. The radar volume scan beginning nearest to the analysis time is used, given a window of + or − 30 min. Aircraft reports are currently subject to a time window of +15 to −60 min. Shorter windows may be employed if the LAPS analysis cycle time drops below 30 min. No temporal weighting is performed for data occurring within the time window.

The observation residuals are subjected to a quality control check of the magnitude

of the difference from the background using a threshold that depends on the data source. Currently, the empirically determined thresholds are 15 m s^{-1} for profilers, 12 m s^{-1} for Doppler radial velocities, 10 m s^{-1} for aircraft winds, and 30 m s^{-1} for other data sources. An additional quality control check for ACARS data compares the aircraft tail number to a list of aircraft with known problems. Observations from these aircraft are rejected.

The u and v wind components are analyzed independently. The residuals are first mapped onto the nearest grid point in three dimensions. The residuals (excluding those from radar and profiler observations which are already sufficiently dense in the vertical direction) are next spread by duplicating the value of the residual vertically onto grid points within 50 hPa of the observation's level. An empirical vertical weighting term v, depending on how far the observation has been spread in the vertical, is given by

$$v = e^{-(\frac{z}{r_v})} \tag{1}$$

where z is the vertical distance and r_v is 25 hPa or 0.5 vertical levels. The term applies to the weight given the observation rather than the magnitude of the observation residual. The nonradar observations are spread up and down by 50 hPa if no prior observation exists at the vertically adjacent grid point. A simple objective analysis scheme is used to analyze these residuals onto the LAPS grid as described next.

The observations are analyzed level by level. A Barnes (1964) exponential weighting is used where the radius of influence is a spatially varying function of the data density. For each grid point, each observation is given a weight w as follows:

$$w = vte^{-(\frac{s}{r_h})^2}. \tag{2}$$

Here, v is the vertical weighting term, t (normally 1) is defined by the data type, and s is the distance (measured in grid points) of the observation from the data point in question. The horizontal radius of influence r_h (in units of horizontal grid increment) is obtained empirically as follows:

$$r_h = 1.7\sqrt{\frac{1}{d}}. \tag{3}$$

The data density d is expressed as the fraction of grid points in the local area having an observation mapped onto them. The grid is first subdivided into 6 x 6 grid point boxes. The horizontal radius of influence is determined by counting the number of observations in each 6 x 6 grid point box, applying Eq. 3, then bilinearly interpolating r_h to the entire grid. The horizontal radius of influence is not allowed to exceed 12 grid increments. The variable radius of influence allows the analysis to represent meteorological details appropriate to the data present across the domain despite a strong spatial variability in the data density. For example, dense radar data or mesonet observations may be available in only a part of the domain. Data at very high levels may be fairly dense with aircraft observations,

whereas, in fair weather, middle levels of the atmosphere may only have the relatively sparse profiler or aircraft observations.

The second pass (looping once more around Fig. 3) is similar to the first except that Doppler radial velocities are now used as a source of data. The advantage of incorporating radar data is twofold. First, the radar helps define the large-scale wind field, both with the radial velocities directly and, in the future, when we consider azimuthal variations of radial velocity to retrieve tangential components. The second advantage is in resolving small-scale features, whose detection is important for very short-range forecasting, such as gust fronts, storm-top divergence signatures, and prestorm convergence boundaries.

To generate wind vectors using these radar observations, Doppler radial velocities are mapped onto the LAPS grid. A difference check set at 12 m s^{-1} is used to control the quality of the mapped radial velocities. The radial velocities are dealiased in the LAPS environment by comparing them with the first-pass analysis. For each grid point containing a radial velocity measurement, the tangential wind component is obtained from the analysis performed in the first step. The radial and tangential components are combined to produce a wind vector that can be used in the wind analysis (Fig. 4). For these radar observations, t is given a value of 0.05 and no vertical spreading is performed. This reduced weight has been empirically determined to compensate for the generally greater density of radar observations compared with the other data sources. The analysis increment is then added back to the first-guess analysis to produce the new LAPS wind analysis.

A surface wind field is vertically interpolated linearly in pressure coordinates from the three-dimensional wind analysis. There is currently no explicit frictional adjustment of the winds in the boundary layer. The vertical structure of the boundary layer is depicted to the extent that the model first guess and the observations can resolve it. Obtaining a surface analysis in this manner proves quite useful for depicting winds in the mountainous regions covering a significant portion the Colorado LAPS domain, compared with using surface observations only in a two-dimensional analysis. Profiler, radar, aircraft, and model first guess data are used to infer the surface winds near the mountain peaks, which are above most of the surface stations. These surface winds are separate from those analyzed as part of the LAPS surface package (McGinley et al. 1991). That analysis considers measured pressures and friction in a variational adjustment, but does not utilize profiler, radar, or aircraft data. The two methods of analysis may be combined in the future. Further improvements in boundary layer winds can result from using a mesoscale model for the first guess instead of MAPS (Cram et al. 1993).

5. Derived fields

Inputs for the calculation of derived fields described in this section are illustrated in Fig. 5.

a. *Kinematic vertical velocity*

Vertical velocity is derived kinematically from the horizontal wind analysis. The

divergence field is integrated upward level by level to provide vertical velocity. The terrain induced vertical velocity $\omega_{SFC} = V_{SFC} \cdot \nabla h$, where h is the terrain elevation, provides the lower boundary condition on ω. The ω field is sensitive to errors in the boundary layer winds and will hopefully be improved in the future. The LAPS terrain is the mean elevation in the box immediately surrounding each grid point followed by a 4 δx smoother.

b. *Layer mean wind and storm motion*

Layer mean wind vectors (surface to 300 hPa) are calculated using mass weighted averaging. A storm motion field is calculated by combining the layer mean wind field with storm centroid tracking vectors, as further described in Jackson and Albers (1992). Where convective echoes of at least 30 dbZ were present, then storm centroid tracking vectors were used to represent the storm motion winds. Otherwise, layer mean winds were used. A quality control check compares each storm centroid direction of motion to that of the mean wind. The analysis assigns a constant weight to the mean wind field and a weight inversely related to distance for any storms that are present. This combined wind field is used to advect the radar reflectivity field to provide reflectivity forecasts.

c. *Helicity*

Storm-relative hodographs are evaluated for severe weather potential by calculating a field of storm-relative environmental helicity. Environmental helicity is calculated as shown in Eq. 4, where v is storm relative wind and ω_H is horizontal vorticity.

$$H = \frac{\int_{Z_1}^{Z_2} v \cdot \omega_H}{Z_2 - Z_1} \tag{4}$$

H is the area of the hodograph (Fig. 6) in the storm-relative reference frame per unit of vertical distance (Z). It has dimensions of velocity times vorticity, and is integrated from the surface to 500mb. The storm motion field is described in the previous subsection.

Hodographs with large values of speed shear or veering of wind with increasing height (in the storm-relative reference frame) often have high values of environmental helicity. In such a hodograph, which is favorable for the development of supercellular convection, the horizontal vorticity associated with the vertical shear of the horizontal wind has a component along the horizontal velocity vector (streamwise vorticity, Davies-Jones 1984). The associated vortex lines can then be tilted into the vertical and stretched by updrafts. Using this product, a study could be undertaken to ascertain where in the vertical, relative to cloud base level, large relative helicity values have the strongest association with the occurrence of supercells.

d. *Lifted index times omega*

LI and vertical velocity (ω) are often used individually as precursors of convective development. Surface LI is a good measure of instability with excellent temporal resolution because surface data are rapidly updated. The LI is computed using the LAPS

surface analyses of temperature, dewpoint, and pressure (McGinley 1989). This analysis is designed to yield accurate LIs over varying terrain. Several effects contribute to upward vertical velocity (ω). Surface convergence due to synoptic and-or mesoscale processes is generally dominant on relatively flat terrain. Terrain-induced upslope can occur either as a broad area over smooth inclined terrain or as isolated strong areas over mountains.

A more concise derived field for forecasting convective development is produced by multiplying the surface LI (Doswell 1982) by the vertical motion (ω) at 600 hPa, derived kinematically from the LAPS wind field. The specific formulation uses LI in K and ω in Pa s^{-1}. The product is set to 0 if $\omega > 0$ (downward motion) or LI > 0 (stable air). The upward vertical velocity, ω, is derived kinematically from the LAPS wind field. The combination of these two quantities reveals where an unstable atmosphere is being lifted (Albers 1987,1989). The above listed references discuss lifted index and surface convergence which is closely related to low level vertical motion.

6. Wind analysis verification

The LAPS wind analysis was compared with independent data obtained by the University of Wyoming King Air aircraft flown during WISP91 (Rasmussen et al. 1991). This aircraft flew about 15 research missions within the LAPS domain, recording wind and other data during winter storm conditions generally of the upslope variety. Figures 7a and 7b show scatterplots of the u and v wind components measured for the composite set of aircraft flights for which data are available. The aircraft data are estimated to be better than 1 m s^{-1} in accuracy. The data are filtered to approximately 1000 data points with a 100-s running mean filter; 100-s is about the time it takes for the airplane to fly between two LAPS grid points. This reduces any high-frequency variability unresolvable on the LAPS grid. The vertical clustering of the data indicates individual flight tracks where the aircraft resolved wind structure on smaller scales than LAPS could resolve.

The root mean square (RMS) residuals against these independent data are about 4 m s^{-1} for each wind component. Typical residuals against the dependent data going into the analysis are significantly smaller, as might be expected. A more formal exercise of verification is under way using April 1991 LAPS analyses at FSL. Preliminary results from that study (Cairns et al. 1993) show slightly smaller residuals against independent rawinsonde data and dependent profiler data.

Figures 8a and 8b show scatterplots of the aircraft u and v wind components measured against a "nearest profiler" analysis. The profiler located at Platteville, Colorado was the only data source used with its winds being spread horizontally. Here, the RMS residuals are 0.1 m s^{-1} and 0.3 m s^{-1} greater than in Figs. 7a and 7b, respectively. This result reflects the value added by additional sensors and background model information (in this case, MAPS) relative to a profiler-only analysis.

A more recent study comparing LAPS analyses from July to December 1992, with independent RAOB data is illustrated in Fig. 9. Preliminary investigation of a sounding exhibiting large residuals suggests that the input data (at least at a particular hour) are not

dense enough to resolve many terrain induced circulations. A four-dimensional assimilation featuring model evolution of terrain induced circulations may help in better defining the wind field for this and other cases when the data are relatively sparse.

Other comparisons with "truth" will be performed with various types of sensors being withheld from the analysis. Examination of radial and tangential wind components may help assess the utility of radar data.

7. Extension to multiple radars

The discussion to this point has assumed only one Doppler radar present (at least in any given grid volume). To fully exploit the radar data, we must be able to analyze winds for those grid volumes within range of more than one radar. There are two phases of implementing a multi-Doppler analysis that we have implemented.

The first phase has been tested in a LAPS implementation called Terminal LAPS (T-LAPS) near Orlando, Florida, in conjunction with the Massachusetts Institute of Technology's Lincoln Laboratory (Wilson et al. 1993). This phase is a "multisingle" Doppler approach, which involves successively adding radars to construct wind vectors at each grid point. The more radars we have and the more orthogonal their beams are, the less the insertion algorithm has to rely on the first-pass nonradar analysis for the winds at a given grid point. Observations at those grid points having radar data are initialized with wind vectors from the first-pass wind analysis. The procedure (an iterative application of Fig. 4) specifies that for each radar, the observation is modified by taking the tangential component from the existing vector observation (now acting as the background) and inserting the radial component from that latest radar. This approach has several advantages over traditional dual-Doppler analysis, including a seamless integration of radar with other data sources and smooth transitions between areas within range of one, two, or more radars.

Consider the example of two radars. The background wind modified by the first radar now becomes the background wind when the second radar is operated upon. If the respective radar beams lie at right angles, the derived radar observation becomes equivalent to a dual-Doppler wind vector, with the first-pass analysis contributing no information. If the beams are parallel, the first-pass analysis contributes the tangential component while the second radar dominates by contributing the radial component. Intermediate results occur at other angles and depend on the order in which the radars are considered.

Ultimately, this could be enhanced with a least-squares minimization including all available radars and the nonradar analyzed wind (Fig. 10). Here the difference between the radially oriented components of the analyzed wind and the measured radial velocities (for each radar) are considered along with the deviation of the analyzed wind from the background. The angles formed between the radial beams of the radars are taken into account, with more weight being given when a pair of radar beams are oriented at right angles from the grid point in question. The order of the radars would not be a factor in this approach though one radar could be given more weight than another.

The second phase (Fig. 10) has been implemented by inserting an additional third pass to the analysis, performed between the original first and second passes (Fig. 3). The set of observations for the added pass (now pass two in Fig. 10) includes nonradar data sources, plus observations at those grid points within range of more than one radar. This allows an analysis of nonradar data plus all grid points where the multisingle insertion procedure (beginning with first-pass analysis) utilizes multiple radars illuminating given grid points. This analysis subsequently provides improved tangential wind components to nearby grid points having only one radar measurement available. The multisingle approach still applies where only single Doppler coverage is available, though nearby grid points illuminated by more than one radar now have added influence on what is now the background (i.e., first-pass) wind field. This approach helps avoid rough edges between areas of differing radar coverage, because grid points illuminated by only one radar are more likely to have radial velocities consistent with the more accurate model background.

Consider the following example of how the procedure shown in Fig. 10 is executed. In the first pass, all data sources except the radars are analyzed. In the second pass, the first-pass analysis forms a background and is combined with radar data at those grid points illuminated by more than one radar. These multiple radar observations are used with the nonradar observations to provide the second-pass analysis. The second pass analysis now provides the background for derived radar observations at grid points illuminated by only one radar. Single and multiple radar observations are then used along with the non-radar data for the third-pass analysis. The procedure for the least squares solution of multiple radial velocities plus the background is still being developed at FSL; the multisingle approach described in the first phase can also be used within this particular box on the flow chart.

8. Future work

Future modifications to the scheme shown in Fig. 10. are planned. In one scenario, the output of the previously described analysis could be the input to a variational adjustment. The input winds are variationally adjusted to the radial velocities, as well as possibly some divergence constraints using available meteorological information. Divergence and vorticity information supplied by radar pattern recognition algorithms of both velocity and reflectivity data may also be included as constraints. Phenomena such as gust fronts, wind shift lines, microbursts, and mesocyclones could thus be included here.

Reflectivity fine lines can also be utilized by applying a divergence constraint to the analysis based on measured radial velocities, then reducing its weight in the vicinity of fine lines (which presumably have locally increased magnitude of divergence).

For both velocity and reflectivity examples, the algorithms are allowed to modify the tangential wind field; the radial wind field is still controlled directly by the radial velocities using the "normal" analysis procedure.

Other radar algorithms are potentially capable of producing observations of the tangential wind component in addition to the radial component. Uniform wind techniques

and echo correlation tracking are examples (NEXRAD 1985). Quality control in each of these is challenging and crucial. Uniform wind methods are often subject to vorticity contamination and may not perform well with sparse radar data. Correlation tracking procedures must be able to discriminate reflectivity features moving with the ambient wind from those that are not.

In the long term, we are investigating still other techniques that may enhance the LAPS wind analysis. We are collaborating with the Center for the Analysis and Prediction of Storms (CAPS) to evaluate a range of techniques for introducing Doppler radar data into the analysis. Some of these involve various dynamical constraints and reflectivity tracking schemes. The implementation of LAPS in Oklahoma is termed O-LAPS and has been used in support of the Verification of the Origin of Rotation in Tornadoes (VORTEX) experiment in 1994.

Another avenue of exploration (personal communication with Cole 1993) involves a technique being developed by Lincoln Laboratory that employs a form of optimal interpolation that analyzes information from multiple Doppler radial velocity data along with conventional vector observations. One advantage of this technique is that each radar need only illuminate nearby grid volumes (as opposed to the grid volume in question) in arriving at an analyzed wind at the given grid volume.

The implementations of T-LAPS in Florida, and O-LAPS in Oklahoma represent the first times that WSR-88D Doppler radar data are being utilized in LAPS. We look forward to expanding the use of these NEXRAD radars as more of these radars are outfitted with wideband data interfaces. A number of WSR-88D radars are planned to be fitted with data interfaces for LAPS during 1995.

Adding an additional iteration of the entire wind analysis may improve the fit of the analysis to the surface observations. Here, the entire procedure shown in Fig. 10 would be executed twice, in the second iteration, the analyzed wind feeds back into the first guess.

9. High resolution analysis and modeling

The LAPS wind analysis currently runs at 10-km horizontal resolution. We are testing the analyses on a nested 2-km grid with an update cycle of 5 min. This uses much of the procedure described above, and is in conjunction with T-LAPS as well as the VORTEX experiment at the University of Oklahoma. One of the main challenges of the higher time resolution is deciding on acceptable time windows for the various data sources.

Initial experiments are also under way to use 10-km LAPS analyses to initialize the Colorado State University (CSU) Regional Atmospheric Modeling System (RAMS) model. Two types of four-dimensional assimilation (4DDA) are being tested. In intermittent 4DDA, the RAMS model replaces MAPS wind tendencies in Fig. 10 to produce the background field for LAPS. RAMS is in turn initialized with LAPS. It is hoped that the background field will now have more accurate mesoscale detail. The other scheme involves nudging the RAMS model runs to LAPS analyses in continuous 4DDA. Either way, the

interdependence will give LAPS more credibility as a four-dimensional data assimilation system (Cram et al. 1993).

10. Conclusion

This article describes in detail how the LAPS wind and radar analyses are performed. The LAPS system is a valuable test bed for utilizing many new data sources to provide a coherent picture of atmospheric structure on scales of 2 to 100 km. Real-time analyses have been performed in domains over Colorado, the central United States, and central Florida.

Other work is being done on the LAPS surface analyses as well as cloud and moisture analyses, and modeling in two and three dimensions. During the 1990s, LAPS will continue to evolve into a system that will better serve the needs of operational meteorologists.

11. Acknowlegements

Thanks to John Brown (FSL) who reviewed this paper and gave valuable suggestions.

12. References

Albers, S. C., 1987: A severe weather forecast software package. *Preprints, Tenth Conf. on Probability and Statistics*, Edmonton, Alta., Canada., Amer. Meteor. Soc., 32-38.

Albers, S. C., 1989: A severe weather forecast scheme incorporating mesoscale analyses. *Preprints, 12th Conf. on Weather Analysis and Forecasting*, Monterey, CA, Amer. Meteor. Soc., 242-246.

Barnes, S. L., 1964: A technique for maximizing details in numerical weather map analysis. *J. Appl. Meteor.*, **3**, 396-409.

Benjamin, S. G., T. L. Smith, P. A. Miller, D. Kim, T. W. Schlatter, and R. Bleck, 1991: Recent improvements in the MAPS isentropic-sigma data assimilation system. *Preprints, 9th Conf. on Numerical Weather Prediction*, Denver, CO, Amer. Meteor. Soc., 118-121.

Cairns, M., R. J. Miller, S. C. Albers, D. L. Birkenheuer, B. D. Jamison, C. S. Hartsough, J. L. Mahoney, A. Marroquin, P. T. McCaslin, J. E. Ramer, J. M. Schmidt, 1993: A preliminary evaluation of aviation-impact variables (AIVs) derived from numerical models. NOAA Tech Memo ERL FSL-5, 165 pp. [Available from NOAA Forecast Systems Laboratory, R/E/FS1, Boulder CO.]

Cram, J., J. Snook, S. Albers, and J. McGinley, 1993: A brief description of, and preliminary results from, the LAPS modelling/4DDA system. *Preprints, 5th Conf. on Aviation Weather Systems*, Vienna, VA, Amer. Meteor. Soc., J10-J14.

Davies-Jones, R., 1984: The origin of updraft rotation in supercell storms. *J. Atmos. Sci.*, **41**, 2991-3006.

Doswell, C., 1982: The operational meteorology of convective weather. Volume I: Operational mesoanalysis. NOAA Tech. Memo. NWS NSSFC-5, 172 pp.

Jackson M., and S. C. Albers, 1992: Application of a local data analysis and product system to short-term convective forecasting. *Fourth AES/CMOS Workshop: Forecasting in the Nineties*, Whistler, B.C., Canada, Canadian Air Weather Service, 235-244.

Lipschutz, R.C., E.N. Rasmussen, J.K. Smith, J.F. Pratte, and C.R. Windsor, 1989: PROFS' 1988 real-time Doppler products subsystem. *Preprints, 24th Conf. on Radar Meteorology*, Tallahassee, FL, Amer. Meteor. Soc., 211-215.

McGinley, J. A., 1989: The Local Analysis and Prediction System. *Preprints, 12th Conf. on Weather Analysis and Forecasting*, Monterey, CA, Amer. Meteor. Soc., 15-20.

McGinley J., Albers S., and P. Stamus 1991: Validation of a composite convective index as defined by a real-time local analysis system. *Wea. Forecasting*, **6**, 337-356.

NEXRAD, 1985: Next generation weather radar algorithm report: NEXRAD Joint System Program Office, December, 1985. [Available from NEXRAD Joint System Program Office, Washington DC.]

Pratte, J.F., J.H VanAndel, D.G. Ferraro, R.W. Gagnon, S.M. Maher, and G.L. Blair: NCAR's Mile High meteorological radar. *Preprints, 25th International Conf. on Radar Meteorology*, Paris, France, Amer. Meteor. Soc., 863-866.

Rasmussen, R., M. Politovich, J. Marwitz, W. Sand, J. McGinley, J. Smart, R. Pielke, S. Rutledge, D. Wesley, G. Stossmeister, B. Bernstein, K. Elmore, N. Powell, E. Westwater, B.B. Stankov, and D. Burrows, 1991: Winter Icing and Storms Project (WISP). *Bull. Amer. Meteor. Soc.*, **73**, 951-974.

Wilson, W., R. Cole, J. McGinley, and S. Albers, 1993: Real-time multiple single doppler analysis with NEXRAD data. *Preprints, 26th International Conf. on Radar Meteorology*, Norman, OK, Amer. Meteor. Soc., 460-462.

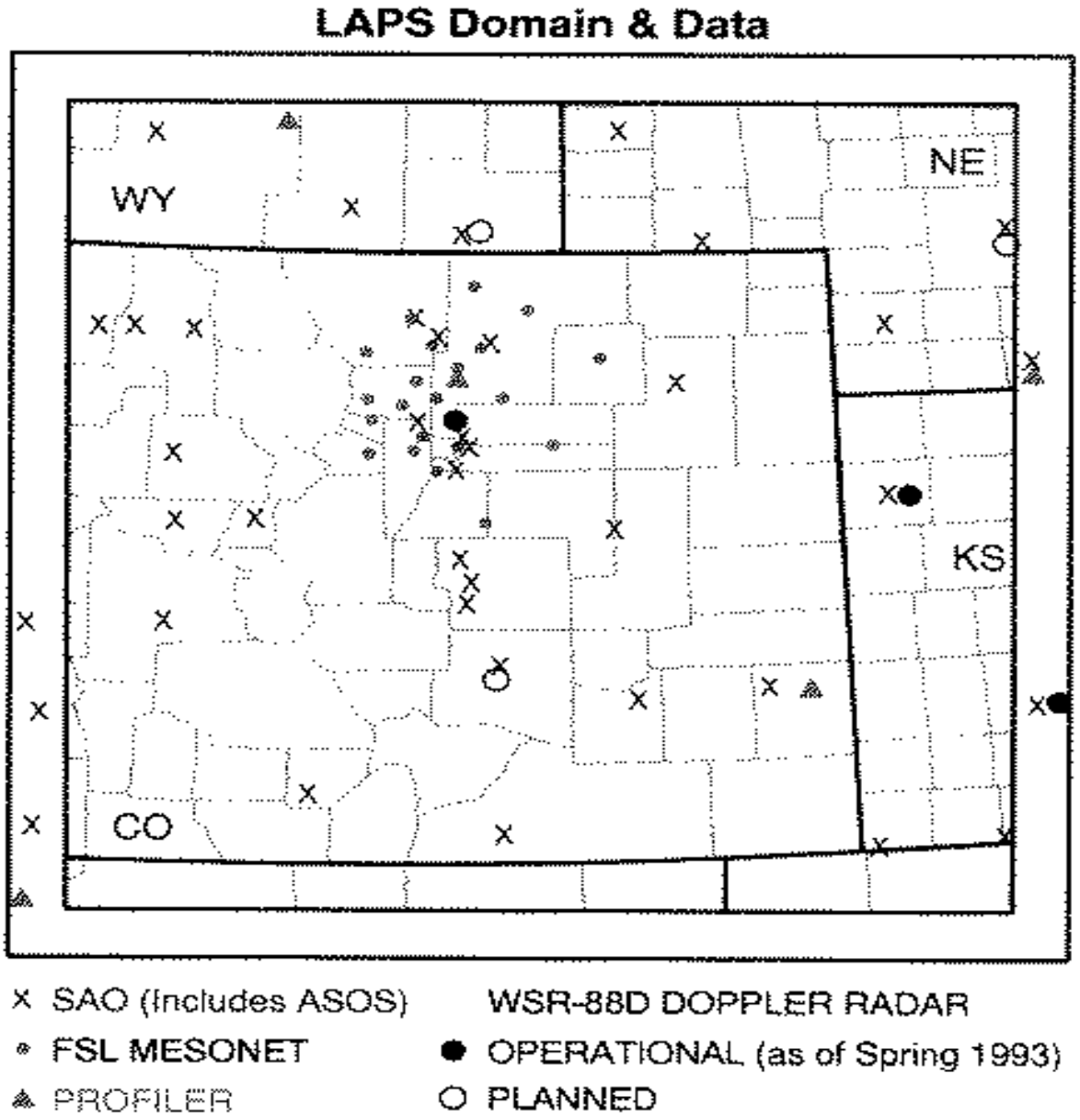

Fig. 1. LAPS domain in Colorado in adjoining states. Various data sources are indicated.

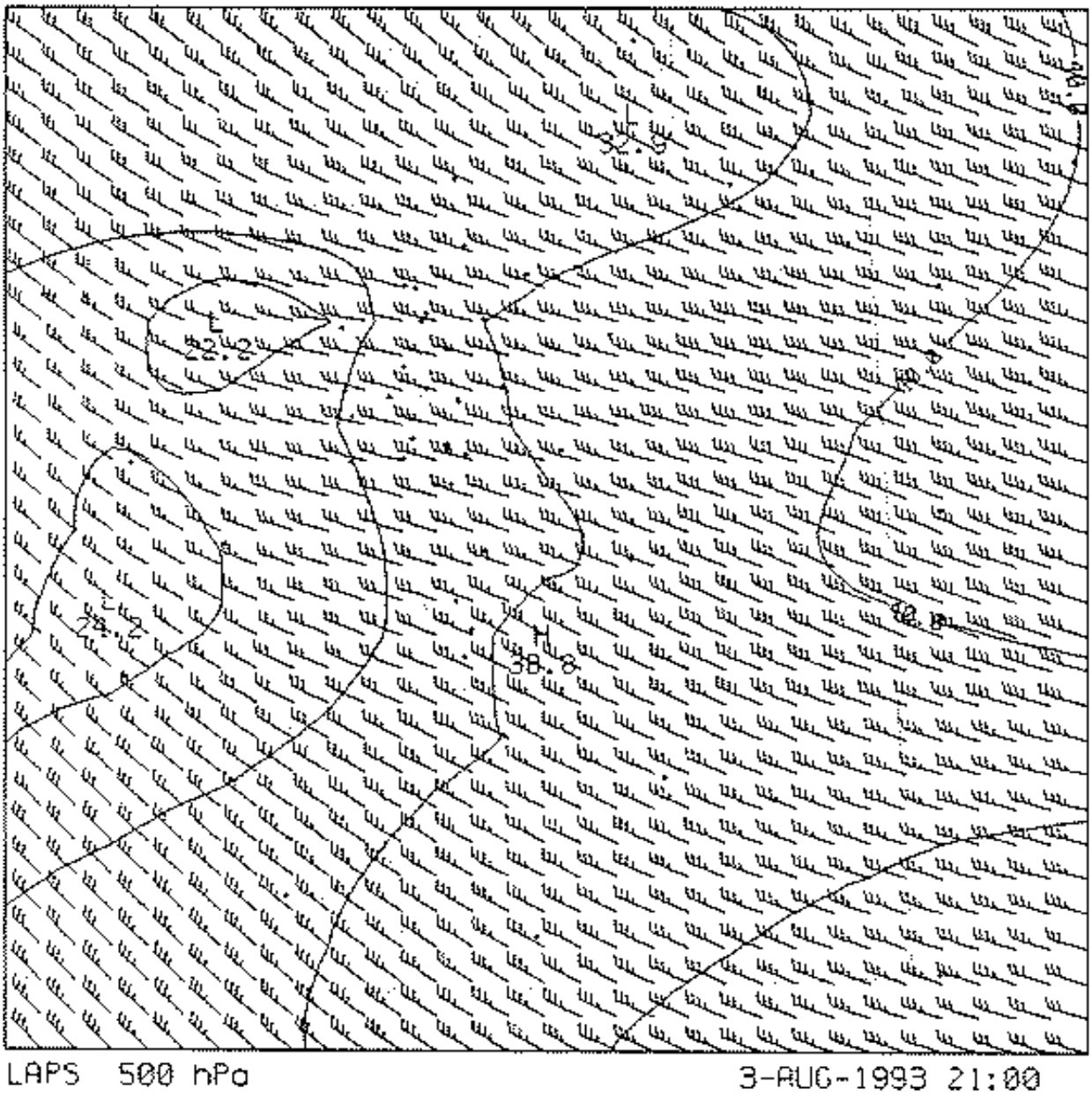

Fig. 2. LAPS wind barbs and isotachs (knots) at the 500 mb level at 2100 UTC, 3 Aug 1993.

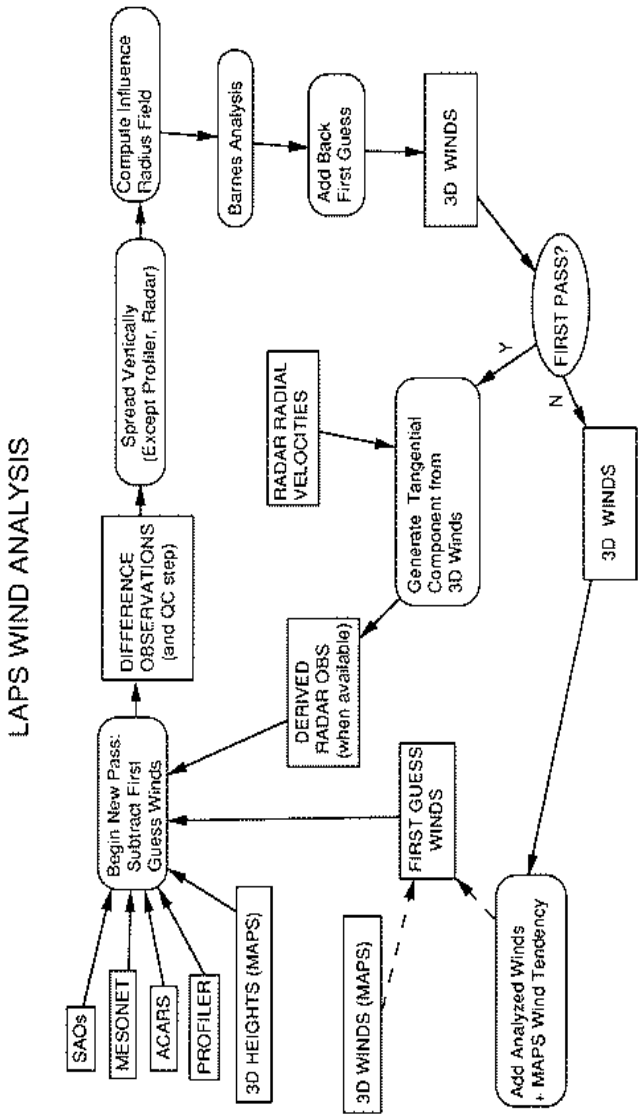

Fig. 3. Flow diagram for producing the LAPS three-dimensional wind analysis. The inputs are SAOs, mesonet winds, pilot reports (PIREPS), wind profilers, and radar radial velocities. Rectangular boxes denote datasets (input, output, or intermediate). Curved boxes represent analysis operations. The dashed arrows represent several possible configurations for generating a first guess wind field, only one is used in any particular analysis cycle.

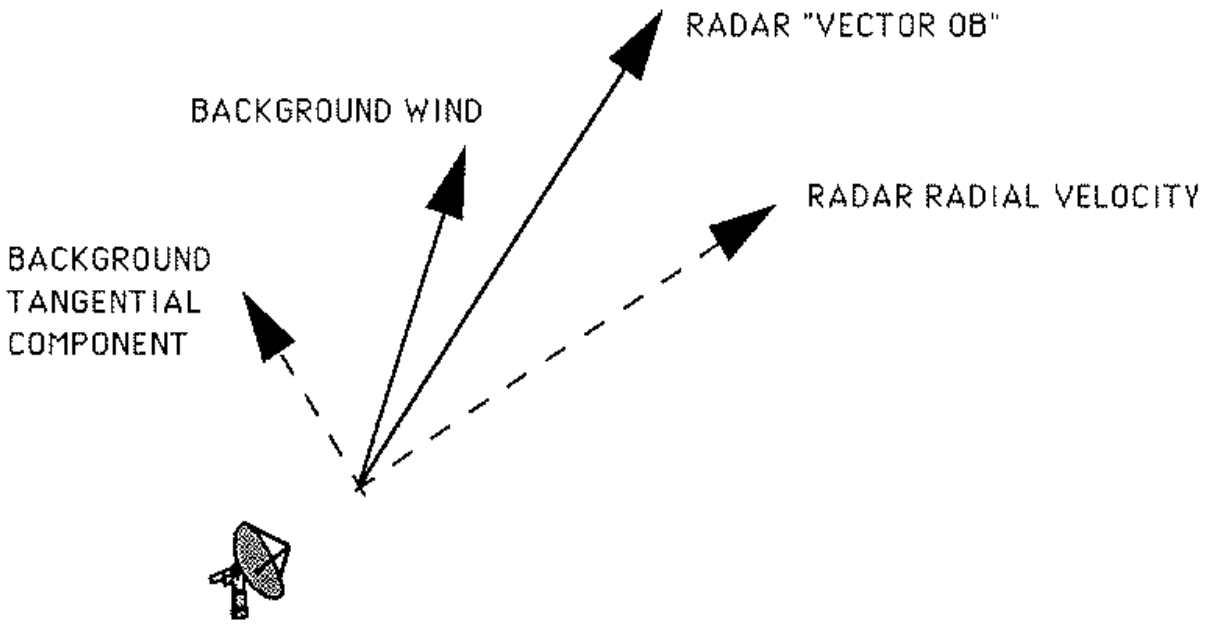

Fig. 4. Illustration of method used to combine the radial velocity from a Doppler radar with the tangential component from a background wind field. The result is a full vector wind observation.

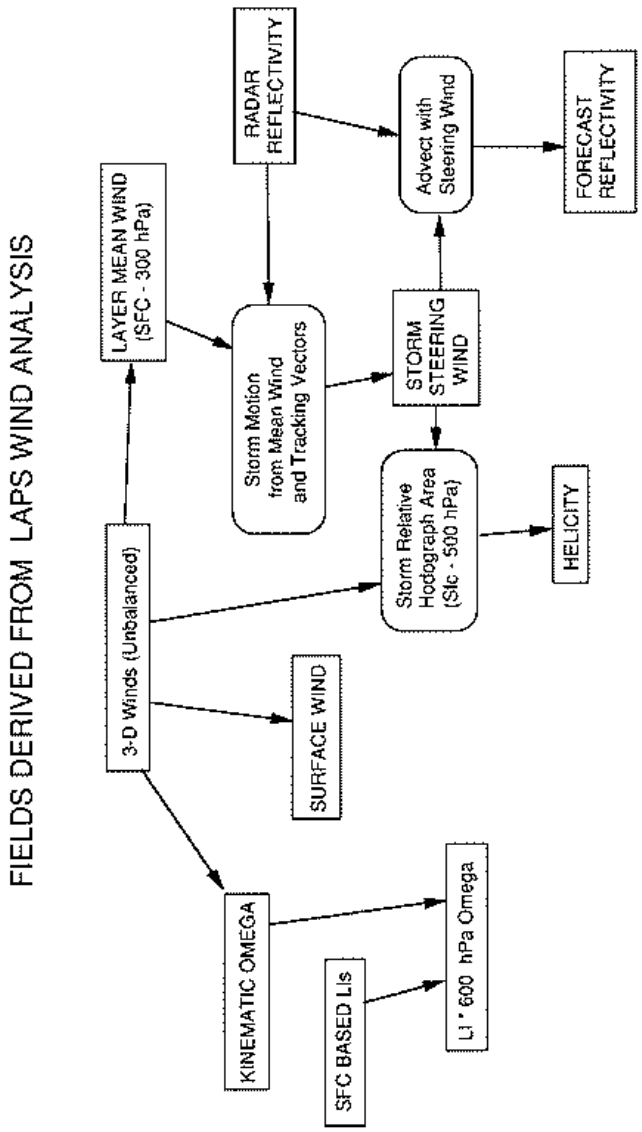

Fig. 5. Flow diagram of various fields derived primarily from the LAPS wind analysis.

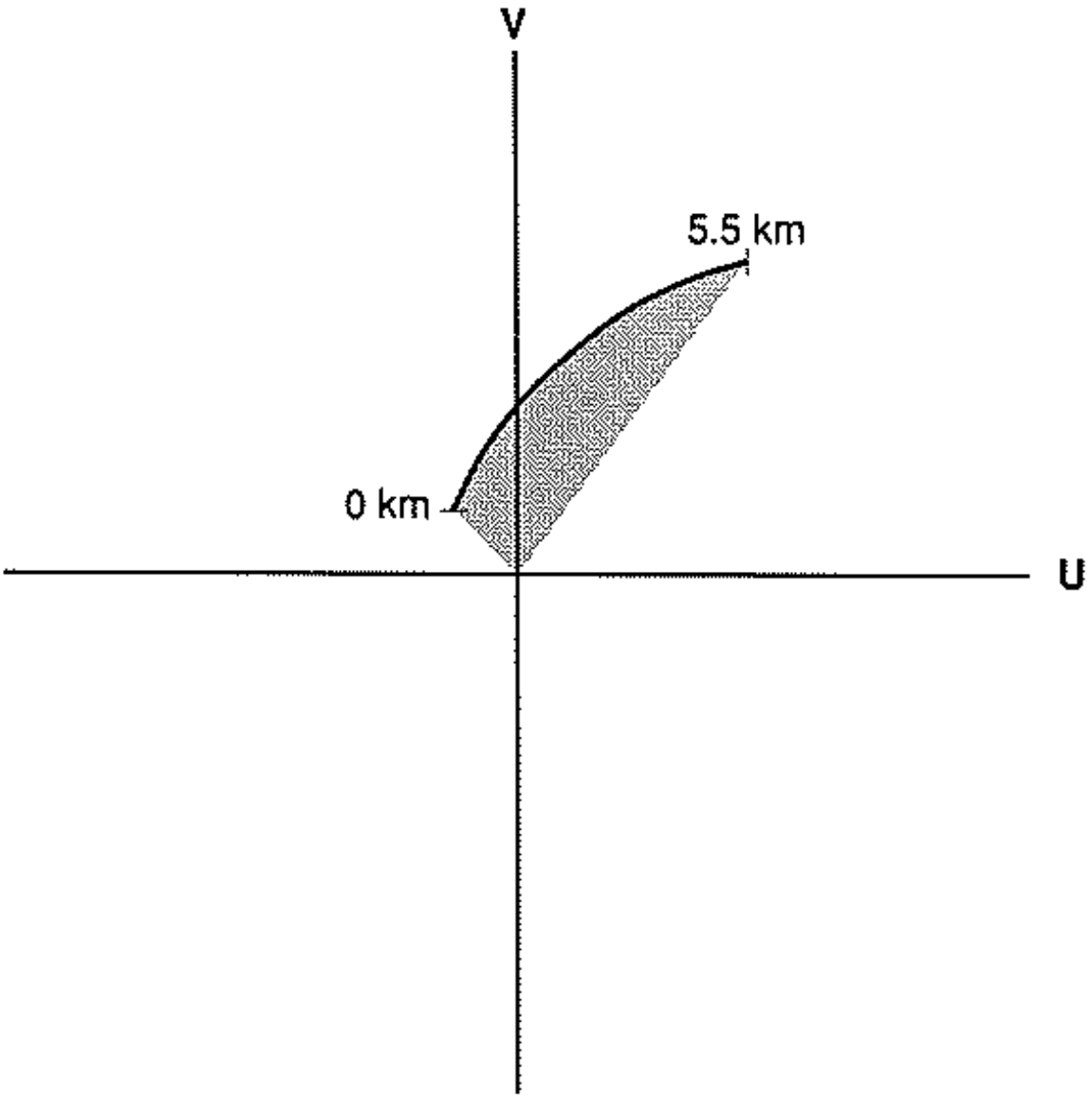

Fig. 6. The area of the hodograph swept out within a layer yields the layer mean environmental helicity. The coordinates represent the storm-relative reference frame. The shaded area in the hodograph represents the helicity in the sounding.

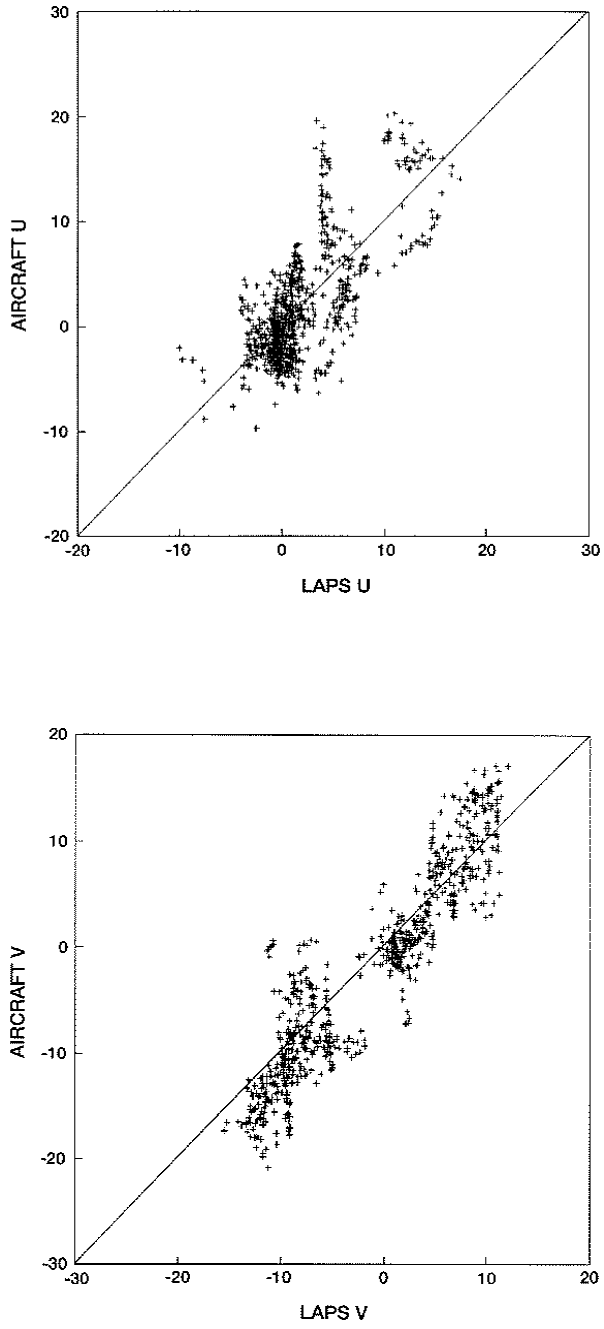

Fig. 7. Scatterplot of u wind component (a) and v wind component (b) as measured by WISP aircraft vs. the LAPS wind analysis interpolated to the aircraft location. Units are meters per second. RMS errors are 4.0 m s^{-1} and 3.7 m s^{-1}, respectively.

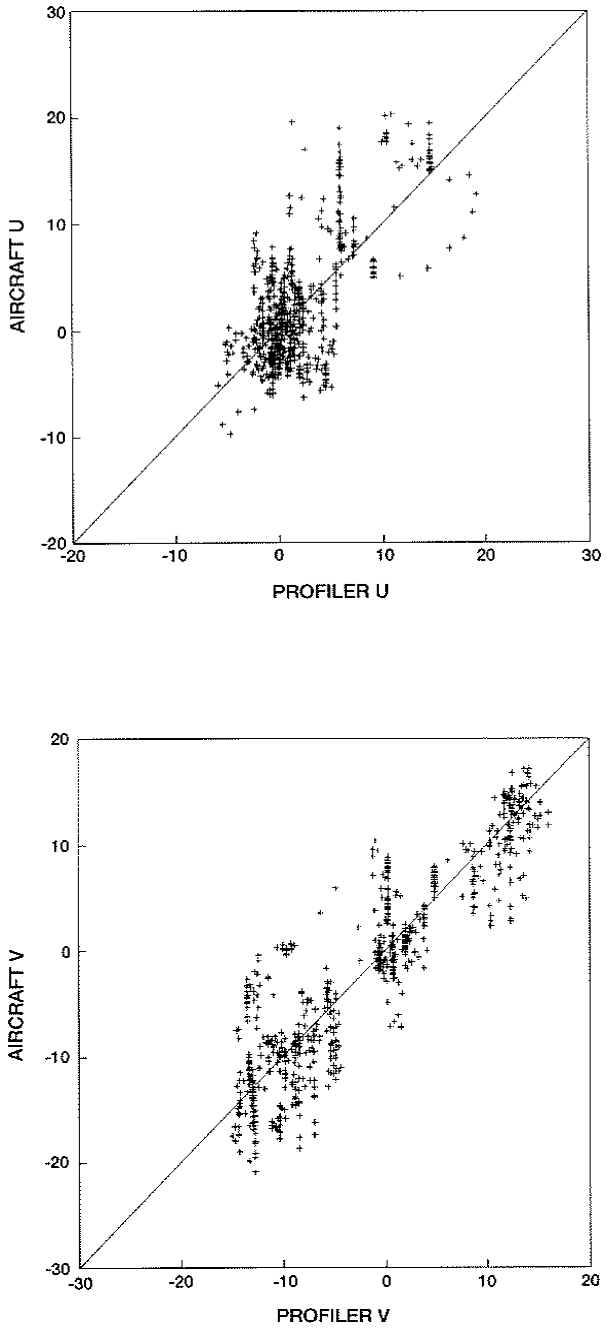

Fig. 8. Scatterplot of u wind component (a) and v wind component (b) as measured by WISP aircraft vs. a simple nearest profiler analysis. Units are meters per second. RMS errors are 4.1 m s^{-1} and 4.0 m s^{-1}, respectively.

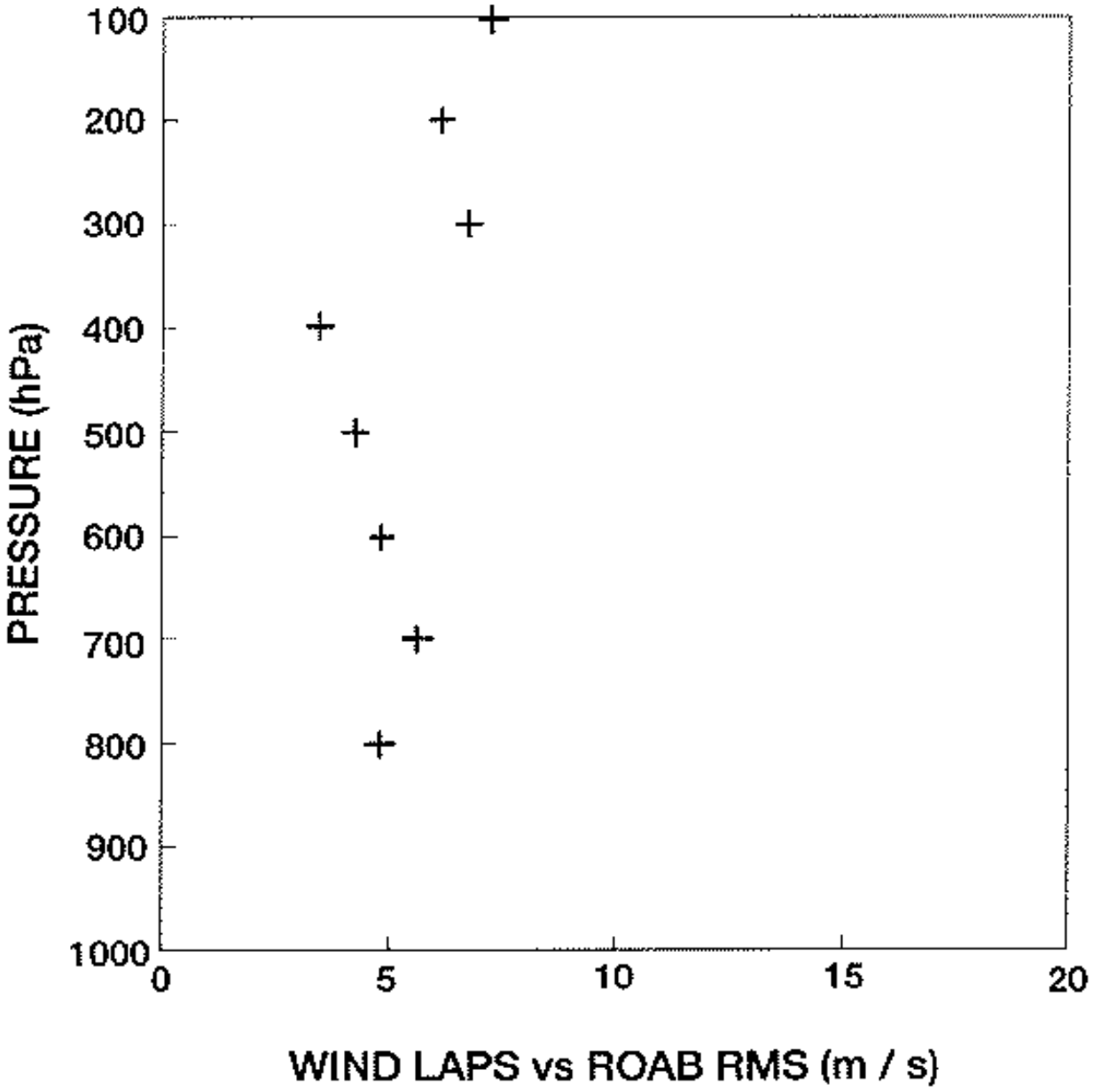

Fig. 9. RMS residuals of LAPS wind analysis compared against independent radiosonde measurements near Denver, Colorado. This represents the aggregate of soundings taken twice daily during approximately the last half of 1992. Units are m s^{-1}.

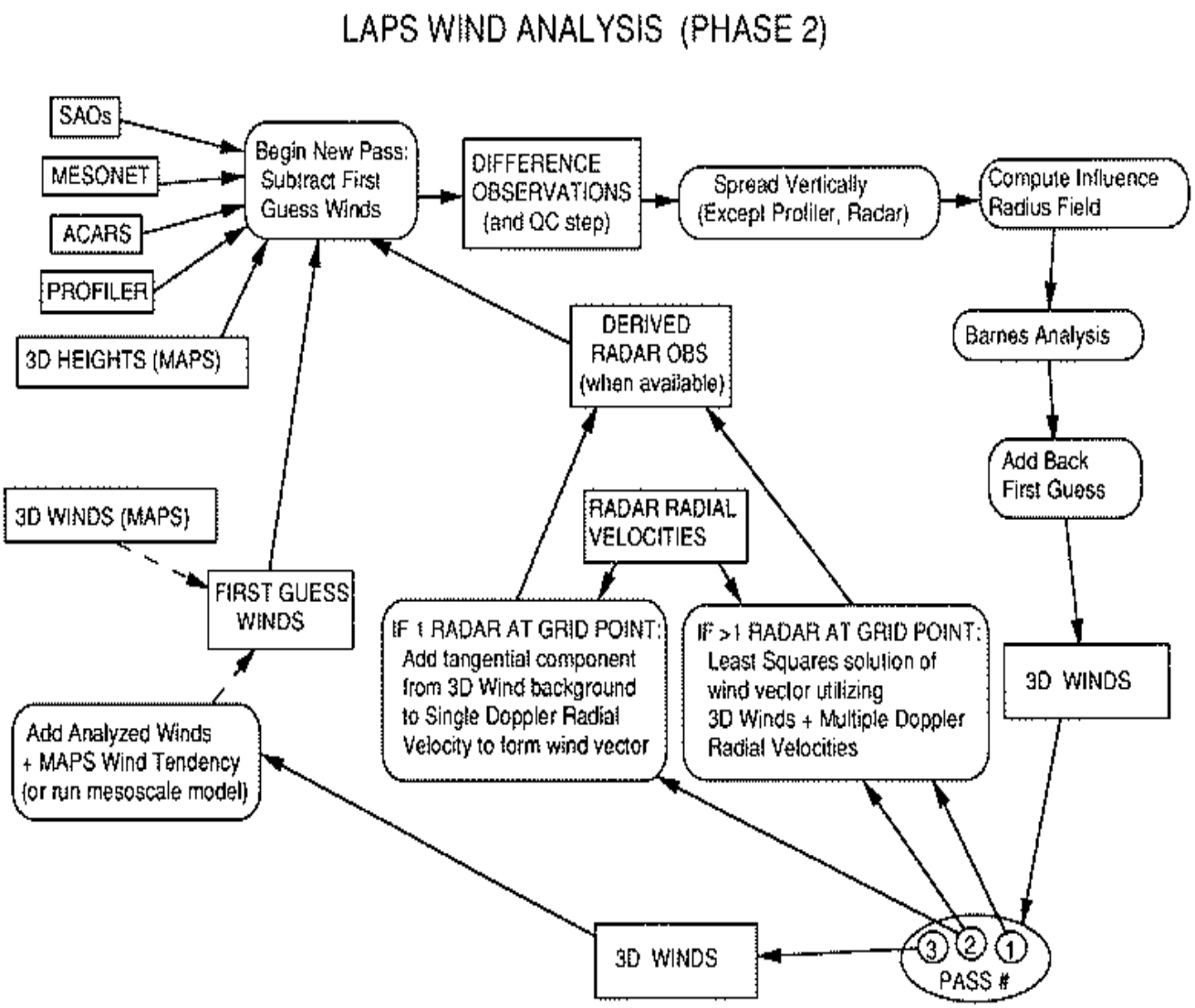

Fig. 10. Modified flow diagram for producing the LAPS three-dimensional wind analysis. A third analysis pass has now been added to better handle the multiple radar situation. The extra pass is used to analyze only those grid volumes illuminated by more than one Doppler radar. Different algorithms are being developed to combine the radar data with the background in the cases of single and multiple radars.